JOURNAL OF APPLIED ELECTROCHEMISTRY 23 (1993) 707–714

Cylindrical three-dimensional electrodes under limiting current conditions

G. KREYSA, K. JÜTTNER

DECHEMA-Institute, Theodor-Heuss-Allee 25, D-6000 Frankfurt am Main 15, Germany

J. M. BISANG

Programa de Electroquímica Aplicada e Ingeniería Electroquímica (PRELINE), Facultad de Ingeniería Química, Universidad Nacional del Litoral, Santiago del Estero 2829, 3000 Santa Fe, Argentina

Received 28 April 1992; revised 22 December 1992

Three-dimensional electrodes of cylindrical geometry, with current and electrolyte flows at a right angle, can be realized with an inner or outer position of the counter electrode. Furthermore, in the case of the fluidized bed the performance of the electrode is also influenced by the position of the current feeder. For the packed bed and the fluidized bed the limiting current analysis has been applied to calculate the variation of overpotential within the bed in relation to the penetration depth of the diffusion limited current density. Results obtained for both cylindrical geometries are compared with those of a rectangular electrode. In the case of a packed bed electrode the largest penetration depth of the limiting current density is offered by the cylindrical design with the counter electrode in an outer position. For fluidized bed electrodes the situation is more complex, depending on the ratio of the solution phase to the particulate phase resistance which is a function of the resistivity and the geometric parameters. However, the configuration with an outer counter electrode is generally more advantageous.

Nomenclature

a_e	surface area per unit volume of electrode (cm^{-1})
E_0	reversible electrode potential (V)
h	electrode length (cm)
i	current density ($A\,cm^{-2}$)
I	total current (A)
L	bed depth for the rectangular arrangement (cm)
r	radius or radial coordinate (cm)
x	axial coordinate for the rectangular arrangement (cm)

Greek characters

δ	ratio between the effective resistivities of the particulate and solution phases
$\Delta\eta$	admitted range of overpotential (V)
$\Delta\phi$	ohmic drop across the electrode (V)
ϵ	ratio between the external and internal radius of the bed
η	overpotential (V)
ρ	resistivity ($\Omega\,cm$)
ϕ	potential (V)

Subscripts

e	external
FBE	fluidized bed electrode
i	internal
L	limit
max	maximum
min	minimum
op	optimum
p	particulate phase
PBE	packed bed electrode
s	solution phase

Superscripts

ICE	inner counter electrode
OCE	outer counter electrode

1. Introduction

Packed and fluidized bed electrodes, also known as three-dimensional electrodes, can be realized by different arrangements with respect to the direction of current flow, electrolyte flow, and electrode positions. The following possibilities exist.

A: Parallel current and electrolyte flow. (There is no principal difference between rectangular and cylindrical arrangements.):

(i) Counter electrode positioned at the current feeder side of the bed electrode;

(ii) Counter electrode positioned opposite the feeder side of the bed electrode.

B: Current and electrolyte flows at right angles:

(i) Rectangular arrangement with a counter electrode positioned at the feeder side of the bed electrode;

(ii) Rectangular arrangement with a counter elec-

0021-891X

trode positioned opposite the feeder side of the bed electrode;
(iii) Cylindrical concentric arrangement with inner position of both the counter electrode and the feeder with a separator between them;
(iv) Cylindrical concentric arrangement with outer position of the counter electrode and the feeder positioned centrally;
(v) Cylindrical concentric arrangement with outer position of both the counter electrode and the feeder with a separator between them;
(vi) Cylindrical concentric arrangement with central position of the counter electrode and outer position of the feeder.

Considering only the one-dimensional model parallel to the current flow direction the cases A(i) and A(ii) are completely similar to the cases B(i) and B(ii), respectively, if a constant concentration of the electroactive species is assumed. A comparative analysis between these cases for the fluidized bed situation has been already given by Fleischmann and Oldfield [1].

Figure 1 depicts the four possibilities of the cylindrical concentric arrangement and also shows schematically the potential distribution for the solution and particulate phases, as well as the overpotential distribution for each case.

Cases B(iii) and B(v) are neglected here because of the high overpotential distribution, which is similar to cases A(i) and B(i). Therefore, the present analysis is focused only on cases B(iv) and B(vi) which present the counter electrode and the current feeder placed in opposite positions with respect to the bed. The equations for B(ii) are dealt with in Section 2.4.

The rectangular and cylindrical arrangements with counter electrode and feeder in opposite positions have been used already for experimental research [2–13]. Theoretical analysis of the potential and the current density distributions, however, is usually restricted to the rectangular design [14–17] although there are some papers [3,18] dealing with cylindrical arrangements. The reason for this situation is that for the cylindrical case the particulate and electrolyte resistances additionally depend on the radius coordinate. However, the cylindrical arrangement is frequently used for practical applications [19–21].

In a previous paper [14] a limiting current analysis for rectangular packed and fluidized bed electrodes was given, resulting in analytical expressions for the penetration depth of the limiting current density (optimum bed depth with respect to the maximum space time yield). It is the purpose of the present paper to derive comparable expressions for both cylindrical cases mentioned above and to discuss some engineering consequences of these calculations.

2. Theoretical considerations

In the following analysis some simplifying assumptions are made:

(i) The main electrode process is a diffusion limited reaction with a current efficiency of 1.
(ii) The microkinetic polarization curve shows a potential range of width $\Delta\eta$; within this the current density varies by less than 1%.
(iii) The whole bed is working under limiting current conditions. This means that at each point the local overpotential lies within the $\Delta\eta$ range, and the full limiting current density is realized.
(iv) Flow velocity is constant over the cross-section (plugflow) and no axial dispersion occurs.
(v) There is no variation of concentration along the coordinate parallel to the current flow direction. This condition is a consequence of assumptions (iii) and (iv).
(vi) In the case of current and electrolyte flows at right angles the two-dimensional situation may be approximated by the one-dimensional model along the current flow direction (x in rectangular geometry and r in cylindrical geometry) applied separately to each point along the flow coordinate. This approach allows the concentration variation in the flow direction to be taken into account.
(vii) The mathematical treatment of fluidized bed electrodes is approached from a macroscopic point of view. Therefore, the model of packed bed electrodes is extended to fluidized bed electodes, which are assumed as the overlapping of two continua: the solution phase and the particulate phase. By analogy with the solution phase, Ohm's law is applied for the particulate phase and thus a proportionality parameter between current density and potential gradient, termed the effective resistivity of the particulate phase, is used. This macroscopic model was used successfully in other work for the correlation of experimental results, the effective resistivity being a fitting parameter. In the present work, the analysis of the mechanisms of charge transfer in the bed is not treated, however this is discussed in the literature [22–26].

The limiting current analysis as characterized by the above assumptions is only an approximate one. However, it is useful due to its simplicity and allows a comparative analysis of different design concepts. It is also the basis of the scale-up of industrial electrolysis cells with three-dimensional electrodes and it has already been successfully applied to the engineering design of waste water purification cells with rectangular geometry [27].

2.1. Cylindrical arrangement with outer counter electrode and inner current feeder (case B(iv))

The differential current balance in the solution phase gives

$$\frac{dI_s(r)}{dr} = i_L a_e 2\pi r h \qquad (1)$$

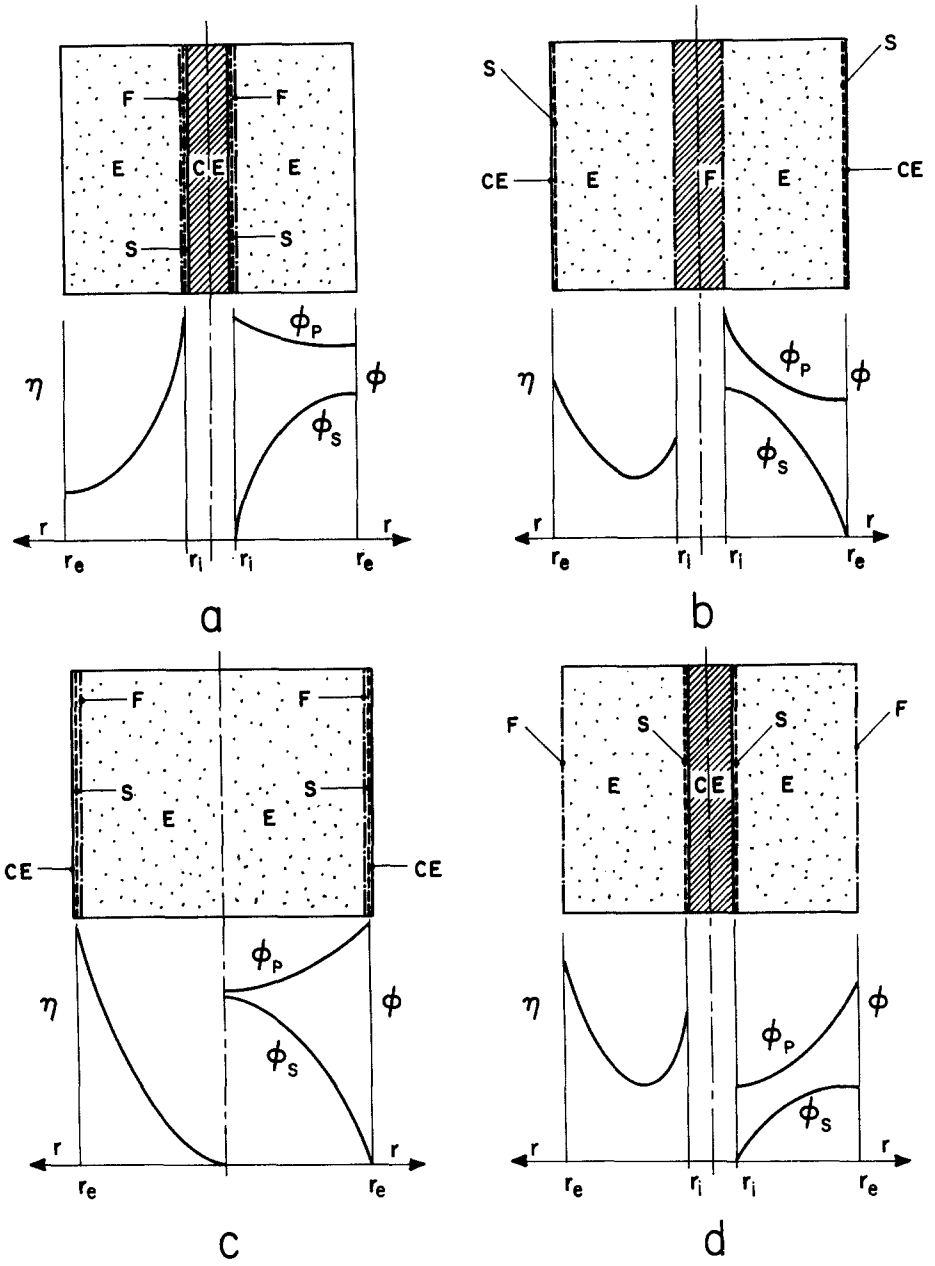

Fig. 1. Schematic representation of various design concepts of three-dimensional electrodes with cylindrical arrangement. CE: counter electrode, E: three-dimensional electrode, F: current feeder of the electrode, S: separator. (a) case B(iii), (b) case B(iv), (c) case B(v), and (d) case B(vi).

Integrating Equation 1 with $I_s(r_i) = 0$ gives

$$I_s(r) = i_L a_e \pi h(r^2 - r_i^2) \tag{2}$$

By definition of current density in the solution phase

$$i_s(r) = \frac{I_s(r)}{2\pi r h} \tag{3}$$

Introducing Equation 2 into Equation 3 and rearranging yields

$$i_s(r) = \frac{i_L a_e}{2}\left(r - \frac{r_i^2}{r}\right) \tag{4}$$

Ohm's law for the solution phase is

$$\frac{d\phi_s(r)}{dr} = -\rho_s i_s(r) \tag{5}$$

Combining Equations 4 and 5 and integrating yields

$$\phi_s(r) = \phi_s(r_i) - \frac{i_L a_e \rho_s}{2}\left(\frac{r^2 - r_i^2}{2} - r_i^2 \ln\frac{r}{r_i}\right) \tag{6}$$

At each radial position in the bed

$$I = I_s(r) + I_p(r) \tag{7}$$

so that

$$\frac{dI_p(r)}{dr} = -\frac{dI_s(r)}{dr} \tag{8}$$

Introducing Equation 1 into Equation 8 and integrating with $I_p(r_e) = 0$

$$I_p(r) = i_L a_e \pi h(r_e^2 - r^2) \tag{9}$$

Taking into account the definition of current density

in the particulate phase, Equation 9 yields

$$i_p(r) = \frac{i_L a_e}{2}\left(\frac{r_e^2}{r} - r\right) \quad (10)$$

Introducing Equation 10 into the Ohm's law equation and integrating, the following equation is obtained for the potential distribution in the particulate phase

$$\phi_p(r) = \phi_p(r_i) + \frac{i_L a_e \rho_p}{2}\left(\frac{r^2 - r_i^2}{2} - r_e^2 \ln\frac{r}{r_i}\right) \quad (11)$$

By definition of overvoltage

$$\eta(r) = \phi_p(r) - \phi_s(r) - E_0 \quad (12)$$

according to Equations 6, 11 and 12 the overpotential distribution is given by

$$\eta(r) = \eta(r_i) + \frac{i_L a_e}{2} \times \left[\frac{\rho_p + \rho_s}{2}(r^2 - r_i^2) - (\rho_p r_e^2 + \rho_s r_i^2)\ln\frac{r}{r_i}\right] \quad (13)$$

This equation presents two maxima at $r = r_i$ and at $r = r_e$ and one minimum of overpotential at

$$r_{min} = \left(\frac{\rho_p r_e^2 + \rho_s r_i^2}{\rho_p + \rho_s}\right)^{0.5} \quad (14)$$

Solving Equation 13 at $r = r_e$ gives

$$\eta(r_e) = \eta(r_i) + \frac{i_L a_e}{2} \times \left[\frac{\rho_p + \rho_s}{2}(r_e^2 - r_i^2) - (\rho_p r_e^2 + \rho_s r_i^2)\ln\frac{r_e}{r_i}\right] \quad (15)$$

There are two possibilities:

2.1.1. $\eta(r_e) > \eta(r_i)$: In this case

$$\eta(r_e) - \eta(r_{min}) = \Delta\eta \quad (16)$$

Combining Equations 13, 14, 15 and 16 and rearranging yields

$$\Delta\eta - \frac{i_L a_e \rho_s r_i^2}{2}\left\{\frac{\epsilon^2 - 1}{2} - (\delta\epsilon^2 + 1)\ln\left[\frac{\epsilon}{\left(\frac{\delta\epsilon^2+1}{\delta+1}\right)^{0.5}}\right]\right\} = 0 \quad (17)$$

where

$$\epsilon = r_e/r_i \quad (18)$$

and

$$\delta = \rho_p/\rho_s \quad (19)$$

Equation 17 is valid when the second term on the right hand side in Equation 15 is larger than zero, i.e.

$$\delta < \frac{2\ln\epsilon - \epsilon^2 + 1}{\epsilon^2 - 1 - 2\epsilon^2\ln\epsilon} \quad (20)$$

For the case of packed bed electrodes $\rho_p = 0$ and Equation 17 yields

$$\Delta\eta - \frac{i_L a_e \rho_s r_i^2}{2}\left(\frac{\epsilon^2 - 1}{2} - \ln\epsilon\right) = 0 \quad (21)$$

2.1.2. When $\eta(r_i) > \eta(r_e)$:

$$\eta(r_i) - \eta(r_{min}) = \Delta\eta \quad (22)$$

Combining Equations 13, 14 and 22 and rearranging gives

$$\Delta\eta + \frac{i_L a_e \rho_s r_i^2}{2}\left[\frac{\delta(\epsilon^2 - 1)}{2} - \frac{\delta\epsilon^2 + 1}{2}\ln\left(\frac{\delta\epsilon^2 + 1}{\delta + 1}\right)\right] = 0 \quad (23)$$

According to Equation 15, Equation 23 is valid when

$$\delta > \frac{2\ln\epsilon - \epsilon^2 + 1}{\epsilon^2 - 1 - 2\epsilon^2\ln\epsilon} \quad (24)$$

Equations 17 and 23 give the same result when $\eta(r_e) = \eta(r_i)$; in this case in the Inequalities 20 or 24 an equal sign must be employed.

2.2. Cylindrical arrangement with inner counter electrode and outer current feeder (case B(vi))

Using the same procedure as in Section 2.1 the following sets of equations are valid for this case. The potential distribution in the solution phase is

$$\phi_s(r) = \phi_s(r_i) - \frac{i_L a_e \rho_s}{2}\left(\frac{r^2 - r_i^2}{2} - r_e^2\ln\frac{r}{r_i}\right) \quad (25)$$

and the potential distribution in the particulate phase is

$$\phi_p(r) = \phi_p(r_i) + \frac{i_L a_e \rho_p}{2}\left(\frac{r^2 - r_i^2}{2} - r_i^2\ln\frac{r}{r_i}\right) \quad (26)$$

To determine the overpotential distribution the following expression can be used

$$\eta(r) = \eta(r_i) + \frac{i_L a_e}{2} \times \left[\frac{\rho_p + \rho_s}{2}(r^2 - r_i^2) - (\rho_p r_i^2 + \rho_s r_e^2)\ln\frac{r}{r_i}\right] \quad (27)$$

obtained by combining Equations 12, 25 and 26 and rearranging.

Equation 27 shows two maxima for the overpotential at $r = r_i$ and at $r = r_e$ and one minimum at

$$r_{min} = \left(\frac{\rho_p r_i^2 + \rho_s r_e^2}{\rho_p + \rho_s}\right)^{0.5} \quad (28)$$

Solving Equation 27 at $r = r_e$ gives

$$\eta(r_e) = \eta(r_i) + \frac{i_L a_e}{2} \times \left[\frac{\rho_p + \rho_s}{2}(r_e^2 - r_i^2) - (\rho_p r_i^2 + \rho_s r_e^2)\ln\frac{r_e}{r_i}\right] \quad (29)$$

Similarly to the former case there are two possibilities:

2.2.1. $\eta(r_e) > \eta(r_i)$: For this and according to Equations 29, 28 and 27

$$\Delta\eta - \frac{i_L a_e \rho_s r_i^2}{2}\left\{\delta\left(\frac{\epsilon^2 - 1}{2}\right) - (\delta + \epsilon^2)\ln\left[\frac{\epsilon}{\left(\frac{\delta+\epsilon^2}{\delta+1}\right)^{0.5}}\right]\right\} = 0 \quad (30)$$

From Equation 29, Equation 30 is valid when

$$\delta > \frac{2\epsilon^2 \ln \epsilon - \epsilon^2 + 1}{\epsilon^2 - 1 - 2\ln \epsilon} \tag{31}$$

2.2.2. When $\eta(r_i) > \eta(r_e)$:

$$\Delta\eta + \frac{i_L a_e \rho_s r_i^2}{2}\left[\frac{\epsilon^2 - 1}{2} - \frac{\delta + \epsilon^2}{2}\ln\left(\frac{\delta + \epsilon^2}{\delta + 1}\right)\right] = 0 \tag{32}$$

Equation 32 is fulfilled when

$$\delta < \frac{2\epsilon^2 \ln \epsilon - \epsilon^2 + 1}{\epsilon^2 - 1 - 2\ln \epsilon} \tag{33}$$

For the case of packed bed electrodes, $\rho_p = 0$, Equation 32 is simplified to

$$\Delta\eta + \frac{i_L a_e \rho_s r_i^2}{2}\left(\frac{\epsilon^2 - 1}{2} - \epsilon^2 \ln \epsilon\right) = 0 \tag{34}$$

Obviously, when $\eta(r_e) = \eta(r_i)$ the same result is obtained from Equation 30 or Equation 32.

2.3. Ohmic drop in the electrode

Another figure of merit in order to compare the performance of three-dimensional electrodes is the ohmic drop across the electrode, which can be expressed as

$$\Delta\phi = |\phi_s(r_e) - \phi_s(r_i)| \tag{35}$$

2.3.1. Outer counter electrode: Solving Equation 6 at $r = r_e$ and introducing into Equation 35 yields

$$\Delta\phi|^{OCE} = \frac{i_L a_e \rho_s r_i^2}{2}\left(\frac{\epsilon^2 - 1}{2} - \ln \epsilon\right) \tag{36}$$

For a packed bed electrode, making the comparison between Equations 36 and 21,

$$\Delta\phi|^{OCE}_{PBE} = \Delta\eta \tag{37}$$

2.3.2. Inner counter electrode: From Equation 25 evaluated at $r = r_e$ and introducing into Equation 35

$$\Delta\phi|^{ICE} = \frac{i_L a_e \rho_s r_i^2}{2}\left(\frac{1 - \epsilon^2}{2} + \epsilon^2 \ln \epsilon\right) \tag{38}$$

Taking into account Equations 38 and 34 it may again be concluded that the ohmic drop in the packed bed electrodes equal $\Delta\eta$.

2.4. Rectangular arrangement with a counter electrode positioned opposite the feeder side of the bed electrode (case B(ii))

For the sake of comparison the equations for the case of a rectangular arrangement are given, with a counter electrode positioned opposite the feeder side of the bed electrode [12,14–16] and with feeder current at $x = 0$

$$\phi_s(x) = \phi_s(0) - i_L a_e \rho_s x^2/2 \tag{39}$$

and

$$\phi_p(x) = \phi_p(0) - i_L a_e \rho_p (Lx - x^2/2) \tag{40}$$

Thus

$$\eta(x) = \eta(0) - i_L a_e \rho_p L x + i_L a_e (\rho_p + \rho_s)(x^2/2) \tag{41}$$

The minimum value of overvoltage occurs when

$$x_{min} = \frac{\rho_p L}{\rho_p + \rho_s} \tag{42}$$

The optimum bed depth can be calculated using the equations:

$$L_{op} = \frac{1}{\rho_p}\left[\frac{2(\rho_p + \rho_s)\Delta\eta}{i_L a_e}\right]^{0.5} \text{ for } \rho_p > \rho_s \tag{43}$$

and

$$L_{op} = \frac{1}{\rho_s}\left[\frac{2(\rho_p + \rho_s)\Delta\eta}{i_L a_e}\right]^{0.5} \text{ for } \rho_p < \rho_s \tag{44}$$

When $\rho_p = \rho_s$, the largest value of the optimum bed depth is achieved. In this case Equations 43 or 44 give the same result:

$$L_{max} = \left(\frac{4\Delta\eta}{i_L a_e \rho_s}\right)^{0.5} \tag{45}$$

Solving Equation 39 at $x = L$, the ohmic drop across the bed is obtained

$$\Delta\phi = \frac{i_L a_e \rho_s}{2} L^2 \tag{46}$$

Introducing Equation 45 into Equation 46 yields for L_{max}

$$\Delta\phi|_{FBE} = 2\Delta\eta \tag{47}$$

The case of a packed bed electrode can be treated by making $\rho_p = 0$ in Equation 44, thus

$$L_{op} = \left(\frac{2\Delta\eta}{i_L a_e \rho_s}\right)^{0.5} \tag{48}$$

Introducing Equation 48 into Equation 46 yields

$$\Delta\phi|_{PBE} = \Delta\eta \tag{49}$$

3. Results and discussion

Figure 2 shows, for the case of outer counter electrode, the ratio between the external and internal radius of the electrode as a function of the dimensionless parameter δ for different values of the effective resistivity of the solution phase. The same applies for the case of the inner counter electrode in Fig. 3. The values of the parameters in Figs 2 and 3 are: $a_e = 30\,cm^{-1}$, $i_L = 5 \times 10^{-3}\,A\,cm^{-2}$, $r_i = 0.5\,cm$ and $\Delta\eta = 0.5\,V$.

The radius r_i should be calculated in order to ensure isopotentiality of the wire [28], used as current feeder or as counter electrode, and taking into account its

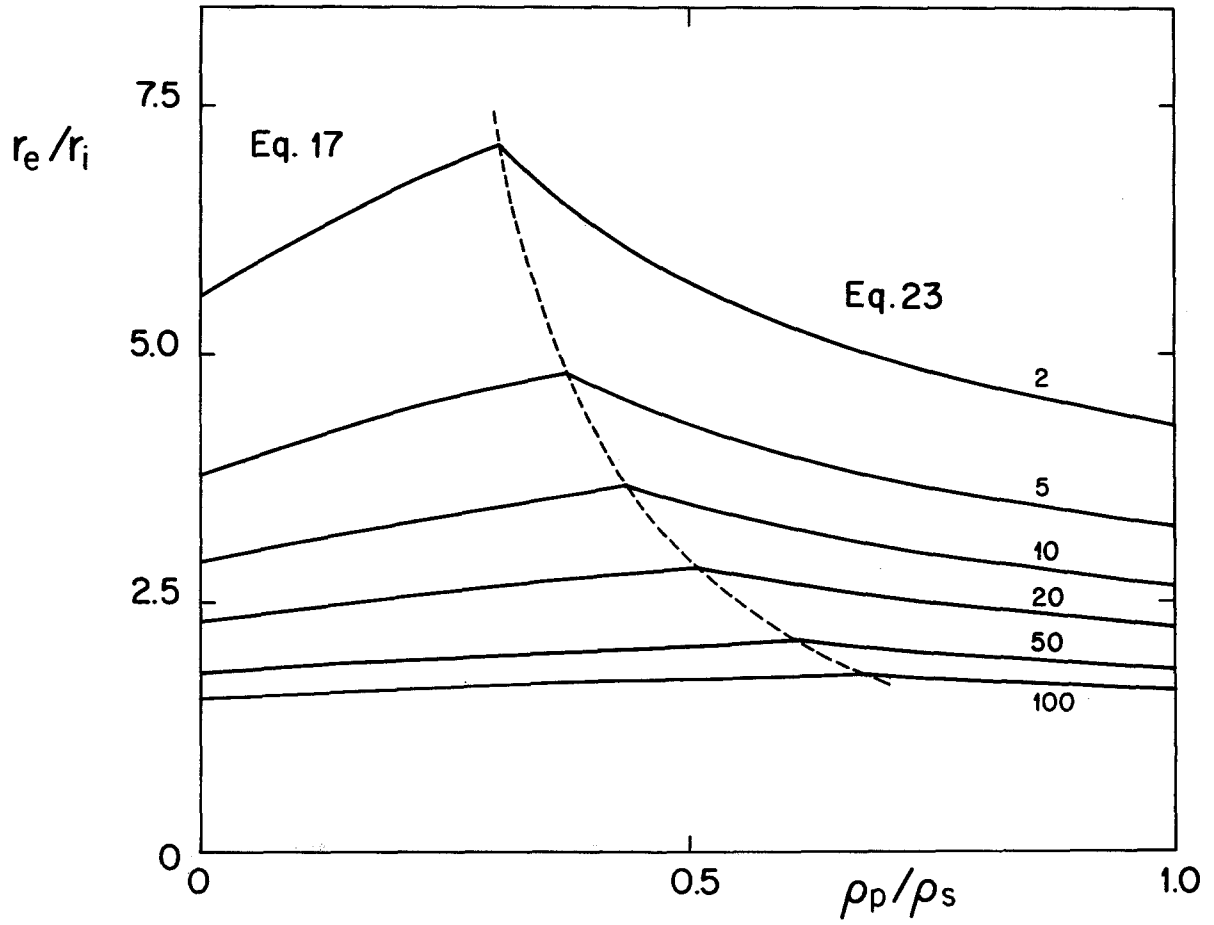

Fig. 2. Ratio between the external and internal radius of the bed as a function of the ratio between the effective resistivities of the particulate and the solution phases. Cylindrical arrangement with an outer counter electrode and an inner current feeder. $a_e = 30\,cm^{-1}$, $i_L = 5 \times 10^{-3}\,A\,cm^{-2}$, $\Delta\eta = 0.5\,V$, $r_i = 0.5\,cm$. The number on each curve corresponds to the effective resistivity of the solution phase and the dashed line represents the limit case of the Inequalities 20 and 24.

mechanical stability. Therefore, in the following discussion r_i is assumed to be known and constant and, consequently, an increase of ϵ means an increase in the bed depth.

The simplest situation is the packed bed electrode, which is represented by the intercept of the curves and the ordinate axis, corresponding to Equation 21 for Fig. 2 and Equation 34 for Fig. 3. In the case of a packed bed electrode the largest bed depth, maximum ϵ, is offered by a cylindrical design with an outer counter electrode and obviously ϵ can be increased when ρ_s is decreased.

When a fluidized bed electrode, with a small value of ρ_p, is used, an active region in the neighbourhood of the current feeder occurs and therefore an increase in ϵ, at the expense of higher values in the ohmic drop, is obtained with respect to the packed bed electrode. Consequently, an increase in ρ_p results in an increase in ϵ. This behaviour is represented by Equation 17 in Fig. 2 and Equation 32 in Fig. 3 and is valid as long as $\eta(r_e) = \eta(r_i)$. In this case, the overpotential at r_i and r_e has maximum value and, therefore, an increase in ρ_p produces a decrease in ϵ due to the fact that $\Delta\eta$ must be constant. This behaviour is shown by Equations 23 and 30 in Figs 2 and 3, respectively.

The dashed line in Figs 2 and 3 joins the points with the largest value of ϵ and in Table 1 the different parameters are summarized when ϵ is maximum.

It is observed that, making a comparison for a given value of ρ_s, the arrangement with an outer counter electrode is preferred because it offers higher values in ϵ, and higher total current, with smaller values in the ohmic drop in the bed. Also Table 1 shows that the configuration with an outer counter electrode

Table 1. Review of the values of merit parameters taken from Figs 2 or 3 where ϵ is maximum

Outer counter electrode

$\rho_s/\Omega\,cm$	δ	ϵ_{max}	$\rho_p/\Omega\,cm$	$\Delta\phi$/V (*Eq. 36*)
2	0.307	7.110	0.61	0.856
5	0.375	4.821	1.88	0.895
10	0.438	3.666	4.38	0.923
20	0.508	2.854	10.16	0.947
50	0.607	2.144	30.35	0.970
100	0.680	1.793	68.00	0.982

Inner counter electrode

$\rho_s/\Omega\,cm$	δ	ϵ_{max}	$\rho_p/\Omega\,cm$	$\Delta\phi$/V (Eq. 38)
2	2.633	4.719	5.27	0.897
5	2.230	3.518	11.15	0.927
10	1.974	2.866	19.74	0.946
20	1.759	2.377	35.18	0.962
50	1.533	1.913	76.65	0.978
100	1.401	1.664	140.1	0.986

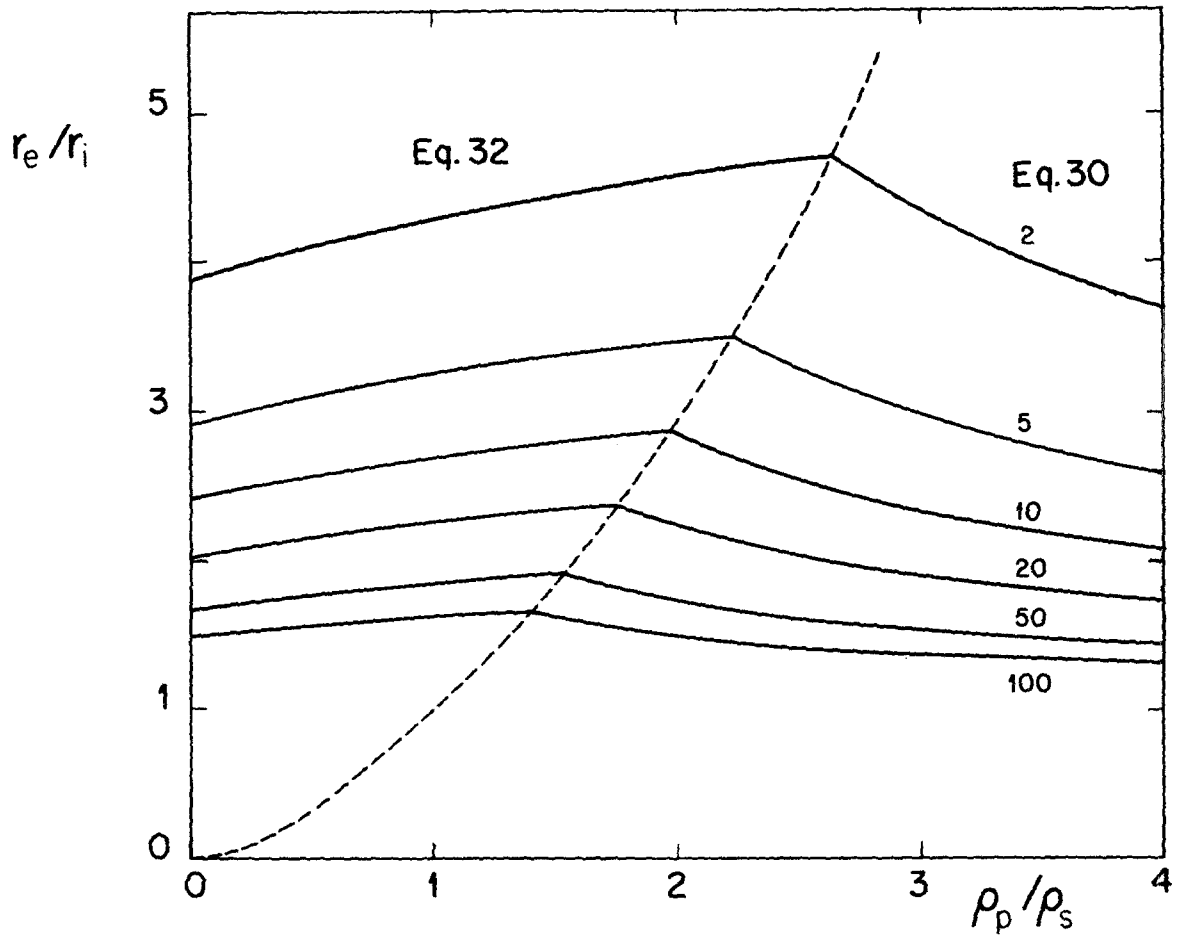

Fig. 3. Ratio between the external and internal radius of the bed as a function of the ratio between the effective resistivities of the particulate and the solution phases. Cylindrical arrangement with inner counter electrode and outer current feeder. $a_e = 30\,cm^{-1}$, $i_L = 5 \times 10^{-3}\,A\,cm^{-2}$, $\Delta\eta = 0.5\,V$, $r_i = 0.5\,cm$. The number on each curve corresponds to the effective resistivity of the solution phase and the dashed line represents the limit case of Inequalities 31 and 33.

presents smaller values in the effective resistivity of the particulate phase, which are in the range of the reported experimental results [29]. This situation can be explained taking into account the influence of geometric parameters, such as the radius, on the resistance of the particulate and solution phases.

When ρ_s increases, as in the case of dilute solutions, the maximum in ϵ shows a tendency to disappear, which is more evident for the arrangement with an outer counter electrode represented in Fig. 2. Likewise, for the higher values of ρ_s both configurations approach the same result.

It must be understood that all the points in the curves of the Figs 2 or 3 have the same space time yield [30]. However, high values in ϵ produce an increase in the total current given by the bed electrode and, consequently, a more efficient utilization of the counter electrode. In the second place, for a required conversion in the reactor, an increase in ϵ allows, for example, a decrease in the number of reactors in parallel at the expense of an increase in ohmic drop calculated from Equation 36 or 38. The optimal value of ϵ must be determined on the basis of economic criteria [31] because a high value of ϵ yields simplified and more efficient construction features and, therefore, produces a decrease in the investment costs, but at the same time it causes a rise in the cost related to the electrical energy consumption.

In Table 2 the cylindrical arrangement with an outer counter electrode and an inner current feeder is compared with the rectangular arrangement with a counter electrode positioned opposite the feeder side of the bed electrode. It can be concluded that for a given value of the effective solution resistivity, the cylindrical configuration is better than the rectangular geometry because the cylindrical arrangement allows larger values of bed depth with smaller values of effective resistivity of the particulate phase and also of ohmic drop across the bed.

In Table 3 the bed depth for both the cylindrical arrangement with an outer counter electrode and the rectangular arrangement for the case of packed bed electrodes is shown. The cylindrical configuration offers the best performance due to the fact that it gives a larger value of bed depth and both geometries have, according to Equations 37 and 49, the same ohmic drop across the bed.

4. Conclusions

The following conclusions may be drawn:

(i) The cylindrical arrangement presents a more complex situation than the rectangular arrangement and the calculation of the bed depth requires a more detailed analysis of effective resistivities of both phases together with geometric parameters.

Table 2. Comparison between the cylindrical and rectangular arrangement in the case of the largest bed depth

Fluidized bed electrode	*Cylindrical arrangement with an outer counter electrode and an inner current feeder*			*Rectangular arrangement with a counter electrode positioned opposite the feeder side of the bed electrode*		
	Case B(iv)			Case B(ii)		
ρ_s /Ω cm	ρ_p /Ω cm	$r_e - r_i\|_{max}$ /cm	$\Delta\phi$ /V (*Eq. 36*)	ρ_p /Ω cm	L_{max} /cm (*Eq. 45*)	$\Delta\phi$ /V (*Eq. 47*)
2	0.61	3.06	0.856	2	2.58	1
5	1.88	1.91	0.895	5	1.63	1
10	4.38	1.33	0.923	10	1.15	1
20	10.16	0.93	0.947	20	0.82	1

Parameters: $a_e = 30\,cm^{-1}$, $i_L = 5 \times 10^{-3}\,A\,cm^{-2}$, $\Delta\eta = 0.5\,V$, $r_i = 0.5\,cm$.

Table 3. Comparison between the cylindrical and rectangular arrangement

Packed bed electrode	*Cylindrical arrangement with an outer counter electrode*	*Rectangular arrangement*
ρ_s /Ω cm	$r_e - r_i$ /cm (*Eq. 21*)	L_{op} /cm (*Eq. 48*)
2	2.29	1.83
5	1.39	1.15
10	0.96	0.82
20	0.66	0.58

Parameters: $a_e = 30\,cm^{-1}$, $i_L = 5 \times 10^{-3}\,A\,cm^{-2}$, $\Delta\eta = 0.5\,V$, $r_i = 0.5\,cm$.

(ii) The cylindrical arrangement with an outer counter electrode (case B(iv)) offers a more advantageous situation than the rectangular configuration (case B (ii)), for both the fluidized bed electrode and the packed bed electrode.

(iii) For cylindrical packed bed electrodes with current and electrolyte flows at right angles the largest bed depth is obtained with an external counter electrode.

(iv) For cylindrical fluidized bed electrodes with current and electrolyte flows at right angles the curves of r_e/r_i as a function of ρ_p/ρ_s, for given values of ρ_s and r_i, show a maximum, which is higher for the case of an outer counter electrode. This maximum represents the best value from the viewpoint of the construction features but the optimization of the bed depth must be made in conjunction with economic criteria.

References

[1] M. Fleischmann and J. W. Oldfield, *J. Electroanal. Chem. Interfacial Electrochem.* **29** (1971) 211.

[2] J. R. Backhurst, J. M. Coulson, F. Goodridge, R. E. Plimley and M. Fleischmann, *J. Electrochem. Soc.* **116** (1969) 1600.

[3] F. Goodridge, D. I. Holden, H. D. Murray and R. F. Plimley, *Trans. Instn, Chem. Engrs* **41** (1971) 128.

[4] S. Germain and F. Goodridge, *Electrochim. Acta* **21** (1976) 545.

[5] F. Goodridge and C. J. Vance, *ibid.* **24** (1979) 1237.

[6] B. J. Sabacky and J. W. Evans, *J. Electrochem. Soc.* **126** (1979) 1180.

[7] W. G. Sherwood, P. B. Queneau, C. Nikolic and D. R. Hodges, *Metall. Trans. B* **10** (1979) 659.

[8] S. Morooka, K. Kusakabe and Y. Kato, *Int. Chem. Eng.* **20** (1980) 433.

[9] A. T. S. Walker and A. A. Wragg, *Electrochim. Acta* **25** (1980) 323.

[10] F. Goodridge, K. Lister and K. Scott, *J. Appl. Electrochem.* **11** (1981) 723.

[11] I. F. Masterson and J. W. Evans, *Metall. Trans. B* **13** (1982) 3.

[12] G. Kreysa and G. Linzbach, *DECHEMA Monographs* **93** (1982) 177.

[13] V. Jiricny and J. W. Evans, *Metall. Trans. B* **15** (1984) 623.

[14] G. Kreysa, *DECHEMA Monographs* **94** (1983) 123.

[15] *Idem*, 'Habilitationsschrift', Universität Dortmund, July (1978).

[16] G. Kreysa, *in* 'Ullmann's Encyclopedia of Industrial Chemistry', **A9** (1987) 204.

[17] F. Coeuret, *J. Appl. Electrochem.* **10** (1980) 687.

[18] B. J. Sabacky and J. W. Evans, *J. Electrochem. Soc.* **126** (1979) 1176.

[19] G. van der Heiden, C. M. S. Raats and H. F. Boon, *Chem. Ind.* **1** (1978) 465.

[20] *Idem, Chem.-Ing.-Tech.* **51** (1979) 651.

[21] L. L. Bott, *Hydrocarbon Proc.* **44** (1965) 115.

[22] M. Fleischmann and J. W. Oldfield, *J. Electroanal. Chem. Interfacial Electrochem.* **29** (1971) 231.

[23] A. A. C. M. Beenackers, W. P. M. van Swaaij and A. Welmers, *Electrochim. Acta* **22** (1977) 1277.

[24] G. Kreysa, *ibid.* **25** (1980) 813.

[25] B. J. Sabacky and J. W. Evans, *Metall. Trans. B* **8** (1977) 5.

[26] R. E. Plimley and A. R. Wright, *Chem. Eng. Sci.* **39** (1984) 395.

[27] G. Kreysa and C. Reynvaan, *J. Appl. Electrochem.* **12** (1982) 241.

[28] J. M. Bisang and G. Kreysa, *ibid.* **18** (1988) 422.

[29] K. Kusakabe, S. Morooka and Y. Kato, *J. Chem. Eng. Jpn.* **14** (1981) 208.

[30] G. Kreysa, *J. Appl. Electrochem.* **15** (1985) 175.

[31] T. Z. Fahidy, *in* 'Principles of Electrochemical Reactor Analysis', Elsevier, Amsterdam (1985) Ch. 11, p. 278.